

EXPERIMENTAL STUDIES ON GÖRTLER VORTICES

S. M. Mangalam
Analytical Services and Materials, Inc.
Hampton, Virginia

J. R. Dagenhart and J. F. Meyers
NASA Langley Research Center
Hampton, Virginia

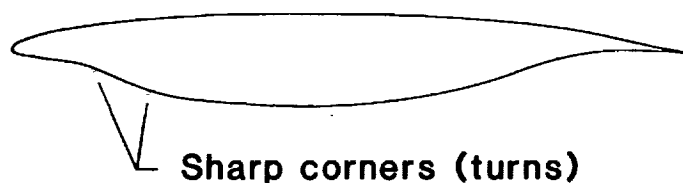
PRECEDING PAGE BLANK NOT FILMED

ABSTRACT

Görtler vortices arise in laminar boundary layers along concave walls due to an imbalance between pressure and centrifugal forces. In advanced laminar-flow control (LFC) supercritical airfoil designs (reference 1), boundary-layer suction is primarily used to control Tollmien-Schlichting instability and cross-flow vortices in the concave region near the leading edge of the airfoil lower surface. The concave region itself is comprised of a number of linear segments positioned to limit the total growth of Görtler vortices. Such an approach is based on physical reasonings but rigorous theoretical justification or experimental evidence to support such an approach does not exist. An experimental project was initiated at NASA Langley to verify this concept. In the first phase of the project an experiment was conducted on an airfoil whose concave region has a continuous curvature distribution. Some results of this experiment have been previously reported (references 2 and 3) and significant features are summarized in this paper. (Figures 1-3).

MOTIVATION

- LFC SC airfoil development
- 8-FT experiment
- Influence of curvature distribution



- Influence of suction
- Study of Görtler vortices in external flow

Figure 1

BACKGROUND

- Previous experiments used "bumps" on opposite walls to ensure attached flow in the concave region or were conducted in channels
- Results indicate invariance of wavelength with freestream parameters
- Information on effects of Suction, Pressure gradient, and Curvature distribution not available

Figure 2

PRESENT EXPERIMENT

- Airfoil model
 - Continuous, smooth curvature distribution
 - Concave region $0.175 < x/c < 0.275$
 - Perforated titanium panel $0.17 < x/c < 0.225$
 - Convex region $0.275 < x/c < 0.50$
- Flow visualization
- Laser velocimetry

Figure 3

AIRFOIL MODEL AND TEST SET-UP

The 1.83-m airfoil model was tested in the NASA Langley Low-Turbulence Pressure Tunnel (LTPT). The model consists of two parts - a structural element and a test insert (Figure 4). With this design several test region geometries can be examined. Attached laminar boundary-layer flow is maintained by means of suction through a perforated titanium panel located in the compression part of the concave region. The suction region is divided into three spanwise suction strips, each controlled independently by its own needle valve. The 10-percent chord flap is used to control the stagnation point location. The experiment was conducted at atmospheric pressure and the chord Reynolds number was varied from 1.0 million to 5.9 million yielding a Görtler number of up to 16.

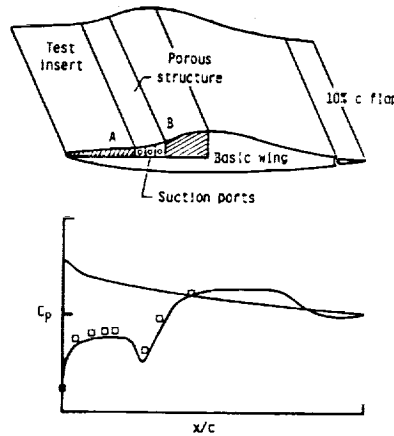
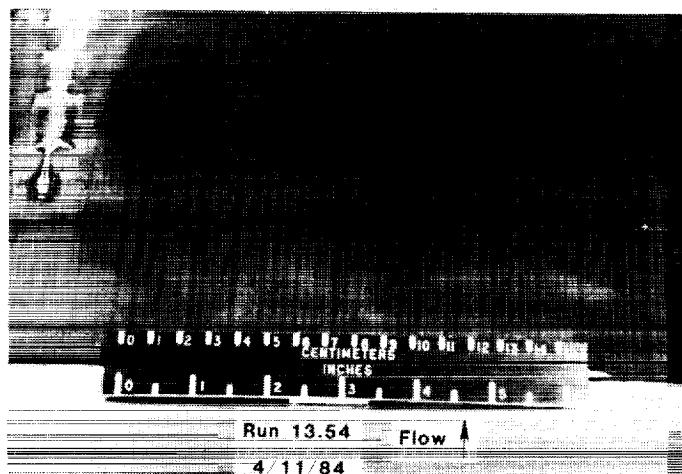


Figure 4

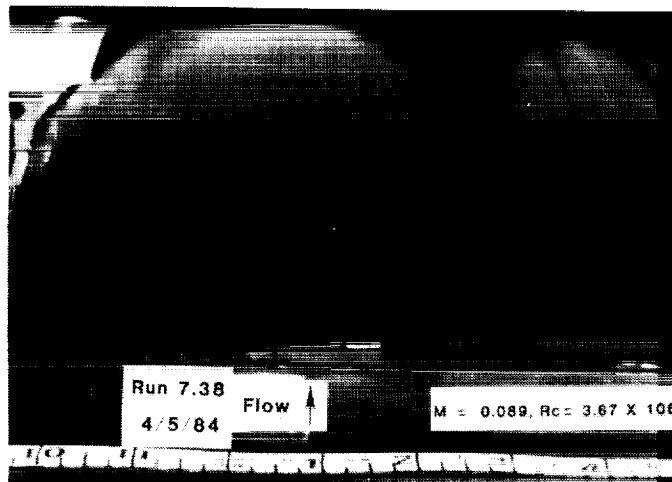
FLOW VISUALIZATION

ORIGINAL PAGE IS
OF POOR QUALITY

A thin layer of solid white biphenyl sublimating chemical was sprayed over the black model surface. The flow pattern is made visible due to the differential surface shear stress distribution under the layer of Görtler vortices which leave behind a trace of alternating white and black bands on the model surface. Elapsed times of about 30 minutes to 1 hour were required for the pattern to emerge clearly. A pair of white and black bands constitutes a wavelength. The wavelength was determined by taking the average of the number of pairs of bands over a 15 cm to 45 cm span. Beyond the concave region, the bands decrease considerably in contrast but are visible back to the jagged transition line. The decrease in contrast is attributed to damping in the convex region. (Figure 5).



$R_c = 2.24$ Million



$R_c = 3.67$ Million

Figure 5

SPANWISE VARIATION OF NORMALIZED STREAMWISE VELOCITY

A specialized, single-axis, three-component laser velocimeter was used to study the flow field in the test region (reference 2). The velocity field was measured by scanning the laser control volume spanwise in steps of 0.05 cm at a constant nominal height above the model surface. The control volume was then moved normal to the surface to the next measurement height and scanned back. This process normally took approximately five hours per chord location. The minimum and the maximum chord Reynolds numbers for laser velocimeter measurements were 1.0 and 3.67 millions, respectively. The spanwise distributions of mean streamwise velocity, normalized with respect to the local boundary-layer edge velocity, are given in Reference 2 for different chord locations and chord Reynolds numbers. Typical results at $x/c = 0.25$ are shown in Figures 6(a) and 6(b) for the lowest and the highest test chord Reynolds numbers. The perturbations are observed to vary across the boundary layer with an essentially constant periodicity along the span for a given chord Reynolds number. Appreciable difference in periodicity is clearly seen with a change in chord Reynolds number. Maximum spanwise fluctuations of as much as 45-percent in streamwise velocity can be observed in Figure 6(b).

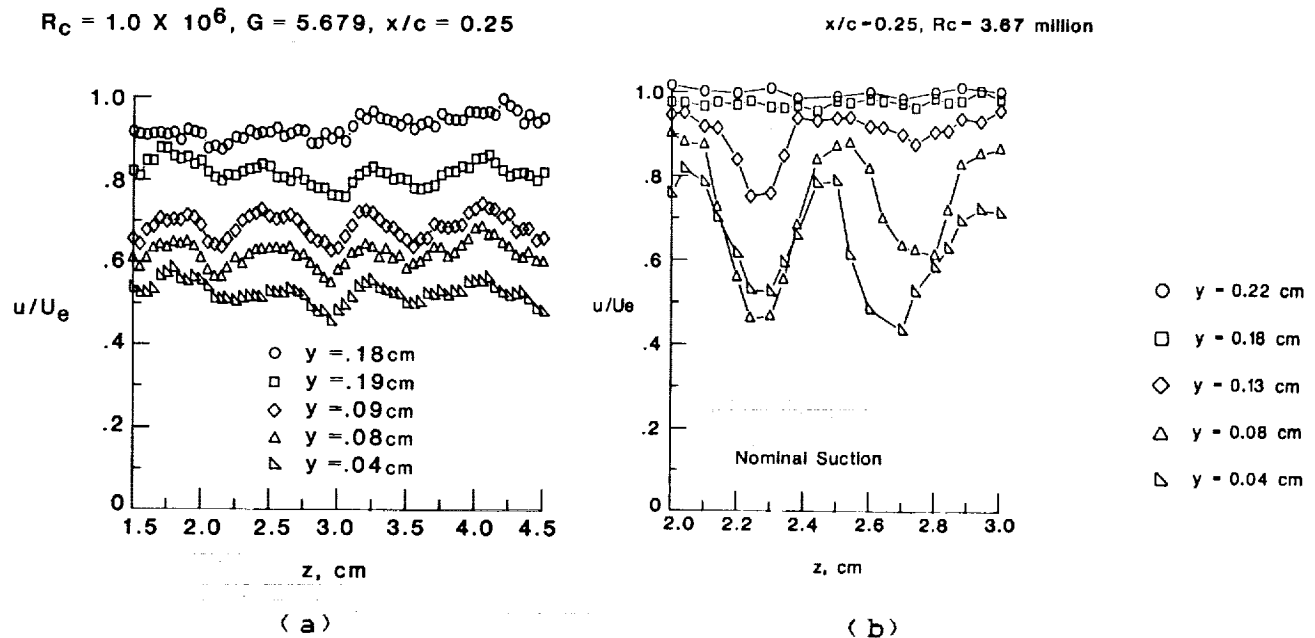
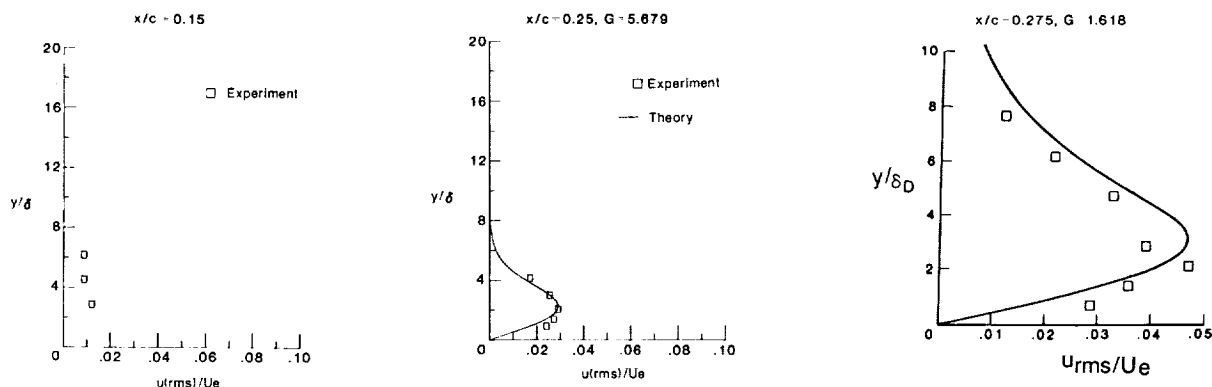


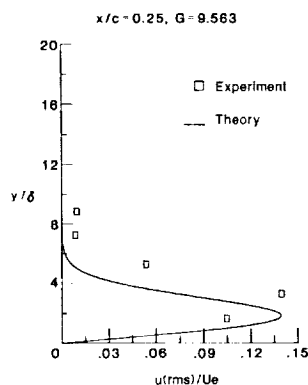
Figure 6

NORMALIZED STREAMWISE VELOCITY PERTURBATION

Normalized streamwise velocity perturbation functions at various chord locations are shown in Figure 7(a) for a chord Reynolds number of 1.0 million. The maximum amplitude of the streamwise perturbation grows to a maximum at the end of the concave region ($x/c = 0.275$) and then falls rapidly in the convex region. Linear theory was used to compute theoretical eigenfunctions corresponding to the measured wavelength. For the purposes of comparison, normalized streamwise velocity perturbation is shown in Figure 7(b) corresponding to chord Reynolds number of 3.67 million. The maximum amplitude reaches a value of nearly 15% of the boundary-layer edge velocity but it is instructive to note that the flow was still laminar.



(a)



(b)

Figure 7

ORIGINAL PAGE IS
OF POOR QUALITY

EFFECTS OF SUCTION

The influence of moderate amounts of additional suction is shown in Figures 8(a) and (b). Nominal suction corresponds to the minimum suction required to maintain an attached laminar boundary layer in the test region. The porous suction strip ends at $x/c = 0.225$ and at this location an increased suction level appears to have consistently reduced the streamwise velocity perturbation. However, at $x/c = 0.25$, where there is no local suction, the streamwise velocity perturbation is consistently larger than those obtained with nominal suction in the compression region. The available results are not sufficient to make major conclusions on the effects of suction. A more detailed study is necessary.

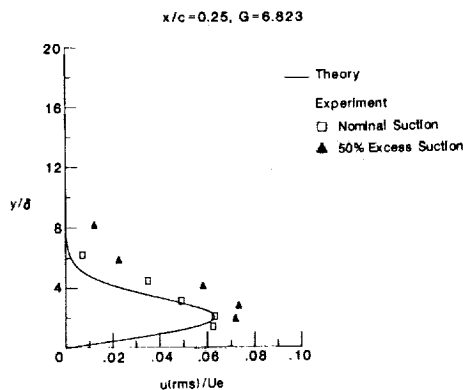
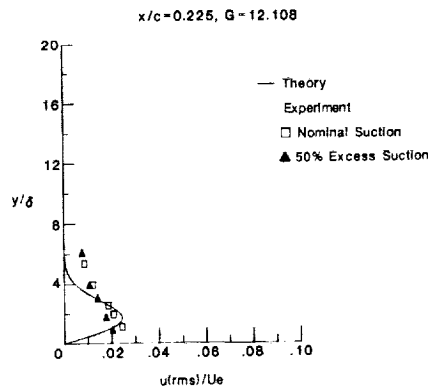


Figure 8

VARIATION IN WAVELENGTH AND MAXIMUM PERTURBATION AMPLITUDE

The variation in wavelength with Görtler number is shown in Figure 9(a). The Görtler number G_m is based on the conditions at the location of the minimum radius of curvature in the concave region. Theoretical results were computed using Floryan's code (reference 4). A good agreement is observed. Unlike all previous experiments, significant variation in wavelength was observed with changes in freestream parameters, as seen from this figure.

The variation in normalized maximum disturbance amplitude is shown in Figure 9(b). Local suction exists in the region $0.17 \leq x/c \leq 0.225$. In this region the growth appears to be gradual but is followed by a sharp increase to the maximum at the end of the concave region. The perturbation amplitudes decrease rapidly in the convex region. Increased levels of suction decrease the amplitude locally but appear to trigger a more rapid growth downstream.

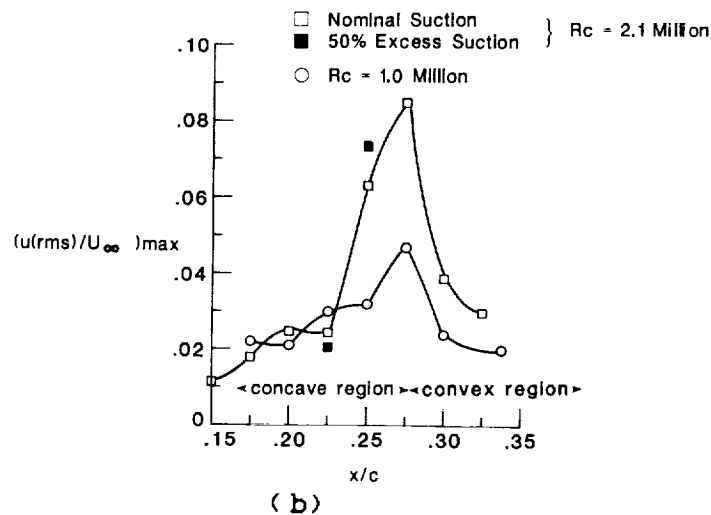
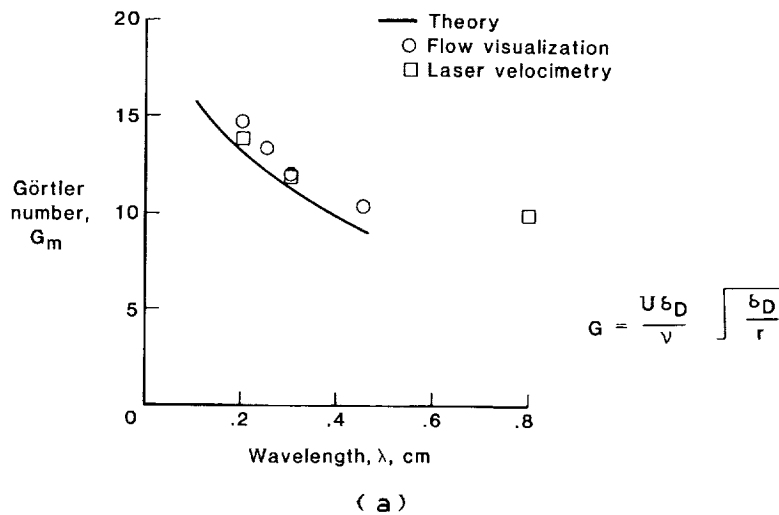


Figure 9

PHASE RELATIONS

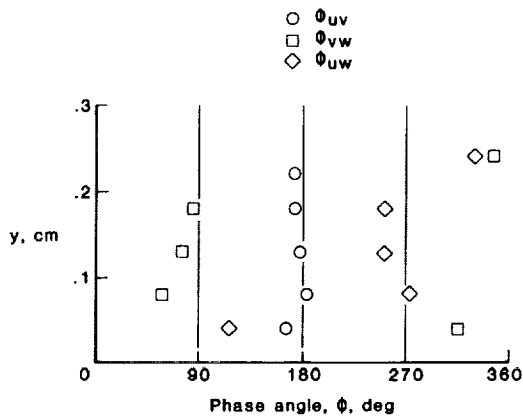
Current theoretical models for velocity perturbations due to the presence of Görtler vortices assume the streamwise and normal velocity components to be in phase and the spanwise component to be out of phase by 90° . However, cross-spectral analysis of experimental data consistently gave results at variance with these assumptions (Figure 10(a)). The streamwise (u) and the normal (v) velocity components were out of phase with each other by 180° whereas the spanwise component (w) was out of phase by 90° or 270° with the streamwise component (270° or 90° with the normal component) depending on the height above the surface. The w -component changes sign across the center of the vortex layer. Such a behavior is consistent with the correct physical model of Görtler vortices shown in Figure 10(b). Based on these results the following correct theoretical model is suggested for velocity perturbations:

$$u(x, y, z) = u(x, y) \cos \alpha z \exp \left(\int \beta_u dx \right)$$

$$v(x, y, z) = v(x, y) \cos (\alpha z + \pi) \exp \left(\int \beta_v dx \right)$$

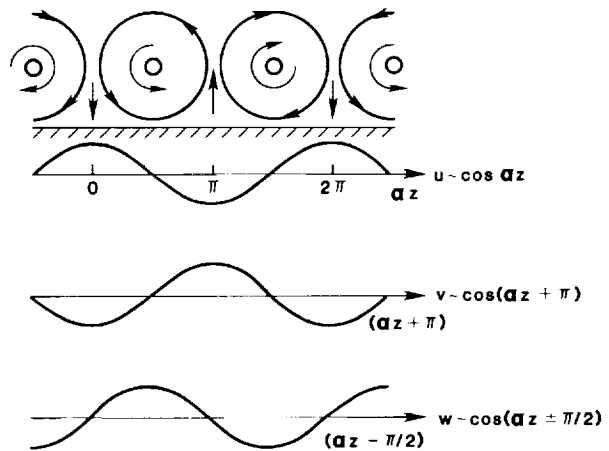
$$w(x, y, z) = w(x, y) \cos (\alpha z \pm \pi/2) \exp \left(\int \beta_w dx \right).$$

MEASURED PHASE RELATIONS
FOR VELOCITY PERTURBATIONS



(a)

PHASE RELATIONS FOR VELOCITY PERTURBATIONS
(Theoretical model)



(b)

Figure 10

SUMMARY OF RESULTS

- Flow visualization and Laser Velocimetry results corroborate dependence of vortex wavelength on freestream parameters
- Measured values agree well with theoretical wavelengths for maximum amplification
- Velocity perturbation profiles determined in the concave and convex regions
- Velocity perturbation profiles and vortex growth trends agree well with theory
- Vortex strength increases in the concave region followed by a rapid damping in the convex region
- Influence of moderate amounts of suction obtained
- Phase relationships between velocity components agree well with the correct physical model

FUTURE EFFORTS

- **More detailed boundary layer measurements to better define stability parameters**
- **Extend the scope of the experiment to study the influence of suction and curvature distribution more thoroughly**
- **Study vortex interaction between Tollmien-Schlichting waves and Görtler vortices**
- **Transition in the presence of Görtler vortices**

REFERENCES

1. Pfenninger, W.; Reed, H. L.; and Dagenhart, J. R.: Design Considerations of Advanced Supercritical Low-Drag Suction Airfoils. In: Viscous Flow Drag Reduction, Gary Hough (ed.), AIAA Progress in Astronautics and Aeronautics, Vol. 72.
2. Mangalam, S. M.; Dagenhart, J. R.; Hepner, T. E.; and Meyers, J. F.: The Gortler Instability on an Airfoil. AIAA Paper No. 85-0491, AIAA 23rd Aerospace Sciences Meeting, Reno, Nevada, January 1985.
3. Dagenhart, J. R.; and Mangalam, S. M.: Disturbance Functions of the Gortler Instability on an Airfoil. ICAS-86-1.8.11, 15th Congress of the International Council of the Aeronautical Sciences, London, England, September 1986.
4. Floryan, J. M.: Stability of Boundary-Layer Flows Over Concave Walls. Ph.D. Thesis, Virginia Polytechnic Institute and State University, Blacksburg, Virginia, January 1980.

